Neural Network Models in EMG Diagnosis

Constantinos S. Pattichis, *Member IEEE,* Christos N. Schizas, *Senior Member, IEEE,* and Lefkos T. Middleton

Abstract— **In the past years, several computer-aided quantitative motor unit action potential (MUAP) techniques were reported. It is now possible to add to these techniques the capability of automated medical diagnosis so that all data can be processed in an integrated environment. In this study, the parametric pattern recognition (PPR) algorithm that facilitates automatic MUAP feature extraction and Artificial Neural Network (ANN) models are combined for providing an integrated system for the diagnosis of neuromuscular disorders. Two paradigms of learning for training ANN models were investigated, supervised, and unsupervised. For supervised learning, the back propagation algorithm and for unsupervised learning, the Kohonen's self-organizing feature maps algorithm were used. Diagnostic yield for models trained with both procedures was similar and on the order of 80%. However, back propagation models required considerably more computational effort compared to the Kohonen's self-organizing feature map models. Poorer diagnostic performance was obtained when the K-means nearest neighbor clustering algorithm was applied on the same set of data.**

I. Introduction

ELECTROMYOGRAPHY (EMG) is the study of the electrical activity of muscle, and forms a valuable aid in the diagnosis of neuromuscular disorders. EMG findings are used to detect and describe different disease processes affecting the motor unit, the smallest functional unit of the muscle. With voluntary muscle contraction, the action potential reflecting the electrical activity of a single anatomical motor unit is recorded. It is the compound motor unit action potential (MUAP) of those muscle fibers within the recording range of the needle electrode [1]. In routine clinical EMG, MUAP morphology is subjectively evaluated by the examiner. However, a purely descriptive approach is not sufficient and an exact quantitative measurement of different MUAP parameters is necessary. Manual quantitative measurement of MUAP parameters was introduced by Buchthal and co-workers in the 1950's and since then, has proven to be a valuable aid in assessing muscle pathology [2]–[4]. However, manual analysis is time-consuming and the subjective measurement of MUAP parameters introduces variable sources of error. Recent advancements in computer technology in the last 20 years have made automated quantitative EMG analysis feasible [5]. Computer-aided EMG processing saves time, standardizes the measurements, and enables the extraction of additional features which cannot be easily calculated manually. To further the development of quantitative EMG techniques, the need has emerged for adding automated decision making support to these techniques so that all data is processed in an integrated environment. Towards this goal, Blinowska [6] proposed the use of discriminant analysis for the evaluation of MUAP findings, Coatrieux and associates [7]–[9] applied cluster analysis techniques for the automatic diagnosis of pathology based on MUAP records, Andreassen and co-workers [10]–[12] developed the MUNIN (Muscle and Nerve Inference Network) which employs a causal probabilistic network for the interpretation of EMG findings, Fuglsang-Frederiksen and his group [13], [14] developed a rule-based EMG expert system named KANDID, and Jamieson [15], [16] developed an EMG processing system based on augmented transition networks. In most of these systems, the generation of the input pattern assumes a probabilistic model, with the matching score representing the likelihood that the input pattern was generated from the underlying class [17]. In addition, assumptions are typically made concerning the probability density function of the input data. Recently, artificial neural networks (ANN) have been proposed as an alternative tool to pattern recognition and classification problems. One of their major advantages is that ANN models make no assumption about the underlying probability density functions of the input data, thus possibly improving the performance of classifiers, especially when the data depart significantly from normality. Other features of artificial neural networks that make them so attractive to investigate are that they: 1) exhibit adaptation or learning, 2) pursue multiple hypotheses in parallel, 3) may be fault tolerant, 4) may process degraded or incomplete data, and 5) seek answers by carrying out transformations.

In this paper, artificial neural networks are used as a new approach for the automatic classification of EMG features recorded from normal individuals and patients suffering with neuromuscular diseases. Two learning paradigms for ANN models are studied: supervised and unsupervised. In supervised learning, the classical back propagation algorithm is used, and in unsupervised learning, the Kohonen self-organizing feature maps algorithm is applied. Performance of neural network models is compared with the K-means nearest neighbor (K-NN) cluster analysis classifier.

II. Method

EMG is recorded from the biceps brachii muscle at slight voluntary contraction for five seconds using the concentric needle electrode. The recording points within the muscle are standardized, with MUAP's recorded from three to five

Manuscript received May 21, 1993; revised January 23, 1995. This work was supported by the Cyprus Institute of Neurology and Genetics (CING) and the University of Cyprus.

C. S. Pattichis and C. N. Schizas are with the Department of Computer Science, University of Cyprus, Nicosia, Cyprus.

L. T. Middleton is with The Cyprus Institute of Neurology and Genetics, Nicosia, Cyprus.

IEEE Log Number 9410031.

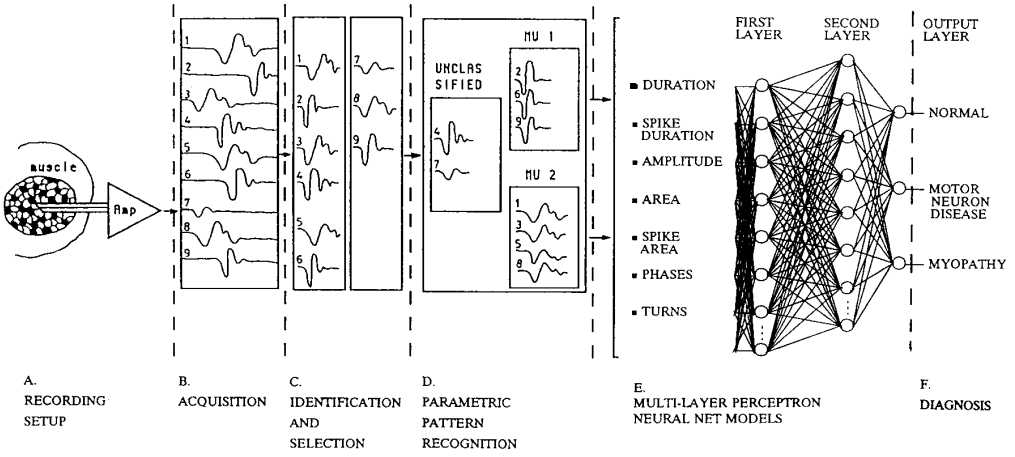

Fig. 1. An integrated system for computer-aided EMG using multilayer neural networks.

different needle insertions. MUAP's are not recorded close to the surface of the muscle. The electrode is usually advanced at least 3–5 mm into the muscle before recording. The electrode is also moved at least 3–5 mm between recordings to make sure that different MUAP's are recorded. The electrode is advanced until the medial or posterior border of the muscle is reached. The electrode is then pulled out to the fascial and inserted to a new radial direction. Usually, one to two MUAP's are simultaneously active within the pick up radius of the electrode. Recording more than two MUAP's simultaneously is more common in pathological cases. For a quantitative EMG study, at least 20 MUAP's are recorded, with the examination procedure taking on average 30–45 min, depending on subject cooperation.

MUAP's are identified and selected from the EMG recording based on predetermined criteria. A parametric pattern recognition (PPR) algorithm based on MUAP features is applied for recognizing similar MUAP's generated from the same motor unit. MUAP features are then applied to a classifier system for obtaining a diagnosis. The proposed integrated system of MUAP analysis [18] follows the path: 1) acquisition, 2) identification, 3) selection, 4) parametric pattern recognition, and 5) neural network models and diagnosis, illustrated in Fig. 1.

A. Acquisition

The EMG signal is freely triggered and a predetermined epoch of five seconds is acquired, bandpass filtered at 3 Hz to 10 KHz, and sampled at 20 KHz with 12 b resolution. The signal is then lowpass filtered at 8 KHz.

B. Identification

A three-step procedure is applied for individual MUAP identification as follows:

1) MUAP extraction. EMG is high-pass filtered at 250 Hz and the MUAP beginning and ending extraction points, BEP and EEP respectively, are identified by sliding an extraction window of length 3 ms and width $\pm$ 40 μV. BEP is the first point that satisfies the following criterion searching to the left of the potential waveform: the signal to the left of BEP remains within $\pm$ 40 μV for 3 ms. EEP is located in a similar way, searching to the right of the potential waveform. These extraction points are then mapped to the original signal.
2) MUAP baseline correction. The average MUAP baseline over 3 ms to the right of point P is computed. This is then subtracted from the potential waveform. Point P is the point which is 6 ms to the left of BEP.
3) MUAP measurement. For each potential the following seven parameters are measured, illustrated in Fig. 2:
   a) Duration (Dur): MUAP beginning and ending are identified by sliding a measuring window of length 3 ms and width $\pm$ 10 μV.
   b) Spike duration (SpDur): measured from the first to the last positive spike.
   c) Amplitude (Amp): difference between the minimum positive peak and the maximum negative peaks.
   d) Area: sum of the rectified MUAP integrated over the duration measure.
   e) Spike Area (SpArea): sum of the rectified MUAP integrated over the spike duration.
   f) Phases (Ph): number of baseline crossings that exceed 25 μV plus one.
   g) Turns (T): number of positive and negative peaks separated from the proceeding and following peak by 25 μV.

The initial part duration is measured from the onset of the potential to the first positive peak. This parameter is used by the pattern recognition algorithm only.

C. Selection

Each individual MUAP is selected for entry to the parametric pattern recognition (PPR) classification process if it satisfies the following criteria:

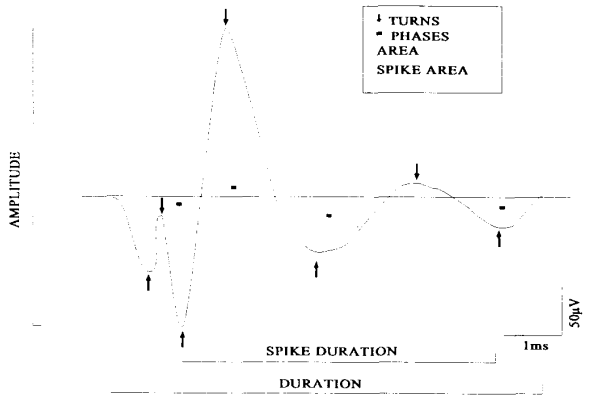

Fig. 2. MUAP parameters.

- Phases ≥ 2.
- Rise time ≤ 1.5 ms (time interval between the minimum positive peak and the maximum negative peak). This criterion is not applied for MUAP's having more than four phases.
- Amplitude ≥ 50 μV.
- 1 ms $<$ Duration $<$ 40 ms (duration upper and lower thresholds were selected to drop potentials with erroneous duration measure entering the pattern recognition algorithm).

D. Parametric Pattern Recognition

The parametric pattern recognition algorithm tries to identify at least three MUAP's which belong to the same group to form a set. The classification is based on five steps where MUAP features: phases, amplitude, spike duration, initial part duration, and duration are examined in sequence [18]. The algorithm is briefly described by the following steps:

1) Step 1. Create Phaseclasses: A Phaseclass is generated by identifying three or more MUAP's that have the same number of phases.

2) Step 2. Create AmpClasses: For each PhaseClass(A) calculate AmpClasses(A) by the following recursive definition:

First the minimum amplitude (MinAmp) is computed. Then, the ExRange set is formed as the collection of MUAPs with amplitude in the range [MinAmp, βxMinAmp] where $\beta = 1.5$. ExRange forms a class if it contains three or more members. MUAP's that do not belong to ExRange set constitute the unexamined set, UnExRange. UnExRange is broken into a new ExRange and a new UnExRange. Then, the MinAmp is calculated for this new ExRange, and the entire process continues as before until the UnExRange becomes empty.

3) Step 3. Create SpDurClasses: This step is implemented in a similar way as Step 2), for the spike duration measure, where β is 1.2. For each AmpClass, SpDurClasses are calculated by the above recursive definition.

4) Step 4. Create InDurClasses: For each SpDurClass, the median of the initial part duration is calculated to decide whether or not the current class under test would be rejected or to continue to Step 5). If there are less than three MUAP's in the class under investigation whose initial duration is not in the range of [$(1-\beta)$xMedian, $(1+\beta)$xMedian], then the current class is dropped for $\beta = 0.2$.

5) Step 5. Create DurClasses: This step is implemented in a similar way to Step 4), for the duration measure, where $\beta = 0.2$.

Usually 20 MUAP sets are collected, and the mean and the standard deviation of the seven parameters are computed to structure a 14-input feature vector. MUAP waveforms and parameters of a normal subject are given in Table I. At the bottom of Table I, the feature vector supplied to the ANN models to provide automated EMG diagnosis is shown.

TABLE I
MUAP PARAMETERS OF AN EMG STUDY OF A NORMAL SUBJECT

MUAP CLASS	N	Dur (ms)	SpDur (ms)	Amp (mV)	Area (mVms)	SpArea (mVms)	Ph	T
1	4	13.00	9.51	0.68	0.48	0.36	4.00	5.00
2	5	11.30	8.96	0.33	0.37	0.29	2.00	2.00
3	3	9.90	2.56	0.41	0.41	0.20	3.00	3.00
4	3	8.80	7.16	0.36	0.37	0.28	2.00	2.00
5	6	9.40	3.34	0.51	0.65	0.42	3.00	3.00
6	8	6.30	6.30	0.07	0.11	0.11	2.00	2.00
7	9	8.60	3.23	0.35	0.44	0.28	3.00	3.00
8	10	7.20	2.85	1.20	0.57	0.41	5.00	5.00
9	4	9.10	3.51	0.15	0.24	0.14	3.00	3.00
10	8	6.80	2.98	1.07	0.56	0.42	4.00	5.00
11	8	7.80	4.44	0.12	0.21	0.12	2.00	2.00
12	6	8.90	5.05	0.68	0.48	0.29	2.00	2.00
13	13	10.20	2.35	1.27	0.69	0.46	5.00	5.00
14	5	14.70	12.96	0.31	0.32	0.27	2.00	3.00
15	4	5.20	5.28	0.32	0.23	0.23	2.00	2.00
16	16	4.70	3.55	0.50	0.18	0.11	2.00	4.00
17	3	9.60	2.68	0.30	0.38	0.16	3.00	3.00
18	3	6.40	4.83	0.10	0.12	0.09	2.00	2.00
19	5	14.20	10.11	0.60	0.69	0.47	2.00	5.00
20	3	8.90	4.63	0.92	0.44	0.30	3.00	5.00
mn		9.05	5.31	0.51	0.40	0.27	2.80	3.30
sd		2.72	2.97	0.36	0.18	0.12	1.01	1.26

E. Artificial Neural Network Models

Two paradigms for training ANN models were investigated, supervised, and unsupervised. For supervised learning, the well-known back propagation algorithm [19], and for unsupervised learning, the self-organizing feature maps algorithm [20] were implemented. Neural network model results obtained with supervised and unsupervised learning paradigms are given in Sections V and VI, respectively. These findings are compared with the results that were given by the K-means nearest neighbor clustering algorithm [21] given in Section IV.

F. Classifier Performance Metrics

For comparing the results that were obtained by the various classification systems, common classifier performance metrics have been used [22]. For a given decision suggested by a certain output neuron, four possible alternatives exist; true positive (TP), false positive (FP), true negative (TN), and false negative (FN). In our study, a TP decision occurs when

TABLE II
MUAP STATISTICS FOR THE NOR, MND, AND MYO GROUPS

	MUAPs	Dur ms		SpDur ms		Amp mV		Area mVms		SpArea mVms		Ph		T	
		mn	sd	mn	sd	mn	sd	mn	sd	mn	sd	mn	sd	mn	sd
NOR	280	9.69	2.64	5.39	2.40	0.37	0.28	0.38	0.19	0.24	0.12	2.6	0.7	3.0	1.0
MND	320	13.10	3.56	6.59	3.09	0.58	0.34	0.77	0.44	0.48	0.27	3.8	1.44	4.45	1.94
MYO	280	7.14	1.91	4.29	1.57	0.31	0.23	0.23	0.14	0.16	0.11	2.7	0.9	3.3	1.2

the positive diagnosis of the system coincides with a positive diagnosis according to the physician. An FP decision occurs when the system made a positive diagnosis that does not agree with the physician. A TN decision occurs when both the system and the physician suggest the absence of a positive diagnosis. An FN decision occurs when the system made a negative diagnosis that does not agree with the physician. From these four measures, the following percentages have been calculated for the N cases in the evaluation set:

$$\%\mathrm{CC's} = 100 \times (\mathrm{TP} + \mathrm{TN})/\mathrm{N}$$
$$\%\mathrm{FP's} = 100 \times \mathrm{FP}/(\mathrm{TN} + \mathrm{FP})$$
$$\%\mathrm{FN's} = 100 \times \mathrm{FN}/(\mathrm{TP} + \mathrm{FN}).$$

Also, the sensitivity SE (likelihood that an event will be detected given that it is present), specificity SP (likelihood that the absence of an event will be detected given that it is absent), recall RE (number of positive diagnoses correctly made by the system, divided by the total number of positive diagnoses made by the physician, where N_{MND} and N_{MYO} are the number of MND and MYO cases, respectively), and precision PR (number of negative diagnoses correctly made by the system, divided by the total number of negative diagnoses made by the physician) are computed as follows:

$$\mathrm{SE} = 100 \times \mathrm{TP}/(\mathrm{TP} + \mathrm{FN})$$
$$\mathrm{SP} = 100 \times \mathrm{TN}/(\mathrm{TN} + \mathrm{FP})$$
$$\mathrm{RE} = 100 \times \mathrm{TP}/(\mathrm{N_{MND}} + \mathrm{N_{MYO}})$$
$$\mathrm{PR} = 100 \times \mathrm{TP}/(\mathrm{TP} + \mathrm{FP}).$$

III. MATERIAL

Neuromuscular diseases are a group of disorders which involves the motor nuclei of the cranial nerves, the anterior horn cells of the spinal cord, the nerve roots and spinal nerves, the peripheral nerves, the neuromuscular junction, and the muscle itself [23]. These disorders cause muscular weakness and/or wasting. From the large number of neuromuscular disorders that have been identified, two groups have been selected for this study, as their consistency of clinical appearance is good. These are motor neuron disease and myopathy.

- *Motor Neuron Disease (MND)* is a disease causing selective degeneration of the upper and lower motor neuron. This disease affects middle- to old-aged people, with progressive widespread loss of motor neurons usually leading to death within three to five years. In the advanced stages of this disease, large motor units also denervate. Motor unit potentials with duration values that are longer than normal and with increased amplitude are typical findings in MND. Their occurrence reflects an increase in the number or density of fibers in motor units, or increased temporal dispersion of the activity picked up by the recording electrode. The latter effect is the result of slowed conduction along the terminal branches of individual nerve fibers, or increase in the end-plate zone, or both.
- *Myopathies (MYO)* are a group of diseases that affect primarily skeletal muscle fibers and are divided into two groups, according to whether they are inherited or acquired. Most muscular dystrophies are hereditary, causing severe degenerative changes in the muscle fibers. In this group of diseases, there are four main types of muscular dystrophy namely Duchenne's, Backer's, fascioscapulohumeral, and limb girdle. They show a progressive clinical course from birth or after a variable period of apparently normal infancy. One of the most frequently acquired myopathies is polymyositis, which is characterized by acute or subacute onset with muscle weakness progressing slowly over a matter of weeks. MUAP's with short duration and reduced amplitude are typical findings in patients suffering from myopathy. These findings are attributed to fiber loss within the motor unit, with the degree of reduction of these parameters reflecting the amount of fiber loss [24].

In this study, a total of 880 MUAP's were collected from the biceps brachii muscle from 14 normals, 16 MND, and 14 MYO subjects. Diagnostic criteria for the subjects selected were based on clinical opinion, biochemical data, and muscle biopsy. Only subjects without a history or signs of neuromuscular disorders were included in the normal group. Furthermore, the biceps brachii muscle was examined because it is a proximal muscle of the shoulder girdle that is usually affected at an early stage in both MND and MYO. Also, its easy accessibility has made it attractive to study and widely reported in the literature.

MUAP findings for the three groups under consideration are given in Table II. Mean and standard deviation of duration of normal subjects are 9.69 $\pm$ 2.64 ms and mean and standard deviation of amplitude is 0.37 $\pm$ 0.28 mV. Myopathy patients usually have MUAP's with short duration, low amplitude, and small number of phases, whereas MND patients have MUAP's with long duration, high amplitude, and a large number of phases. A 2-D scatter plot of the parameters, mean duration, and mean amplitude for each subject is also given in Fig. 3. The complexity of the data under investigation, as illustrated in Fig. 3, shows that no clear boundaries enclosing each group can be drawn.

TABLE III
K-MEANS CLUSTER ANALYSIS PERFORMANCE WHEN MEANS OF SELECTED MUAP PARAMETERS WERE USED

	MUAP Parameters								Training	Evaluation					
	Dur	SpDur	Amp	Area	SpArea	Ph	T	K	%CCs	%CCs	%FPs	%FNs	SE	SP	RE	PR
1	✓							3	83	85	0	21	79	100	79	100
2	✓		✓					3	83	85	0	21	79	100	79	100
3	✓		✓			✓		3	58	50	29	62	38	71	36	71
4	✓		✓			✓		4	83	85	0	21	79	100	79	100
5	✓	✓	✓	✓	✓	✓	✓	3	58	55	17	57	43	83	43	86
6	✓	✓	✓	✓	✓	✓	✓	4	83	85	0	21	79	100	79	100
7*	✓	✓	✓	✓	✓	✓	✓	3	86	85	0	21	79	100	79	100

Number of iterations for all models = 50. *Patient MND1 excluded from the training data set.

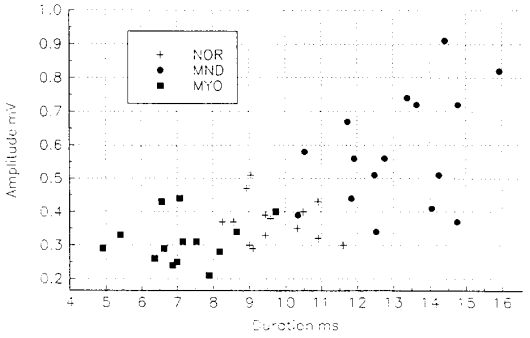

Fig. 3. Two-dimensional scatter plot of mean duration and mean amplitude for each subject.

Twenty-four of the 44 cases in this study have been randomly selected to form the training set (eight subjects from each group), and the remaining 20 subjects were used for evaluating the performance of the models after training. The selection was random, i.e., no criteria were used for assigning a subject either to the training set or to the evaluation set. These sets were used for cluster analysis and for training the back propagation and the Kohonen's self-organizing feature maps models. The mean and the standard deviation of the seven parameters (duration, spike duration, amplitude, area, spike area, number of phases, and number of turns) for each subject were used to structure a 14-input feature vector to be supplied to the learning systems. It has recently been shown that models trained with both the mean and the standard deviation of the EMG parameters produced better results than models trained with only the mean of the parameters [25]. It was concluded that the standard deviation contributes significantly to the learning process.

IV. EMG CLUSTER ANALYSIS FINDINGS WITH THE K-NN ALGORITHM

The K-means cluster analysis algorithm was applied on the training set of patterns to find cluster centers that can be related to disease groups. The cluster centers can be used for checking whether a patient of unknown classification falls into one of the prescribed classes. The algorithm is based on the minimization of a performance index that is the sum of the squared distance from all points in a cluster domain to the cluster center. The behavior of the K-means algorithm is influenced by the number of cluster centers specified, the choice of initial cluster centers, the order in which the samples are taken, and the geometrical properties of the data [21]. In most practical cases, the application of this algorithm requires experimenting with various values of K and different choices of starting configurations. In this study, cluster analysis was carried out on different combinations of MUAP parameters as given in Table III. For model 1, where only the duration feature was used to describe each subject, %CC's for the training and evaluation sets performance were 83 and 80%, respectively. A similar performance was obtained for model 2 when the duration and amplitude parameters were used. In model 3, the parameters duration, amplitude, and phases were used with $K = 3$ (where K is the number of clusters). This model gave poor performance. In this model, cluster 3 has been assigned only to patient MND1. This patient can be considered as an outlier, as it defines its own cluster. However, in model 4, the same parameters were used but K was set equal to four. The percentage of correct classifications increased to 83 and 80%, for the training and evaluation sets respectively. One cluster was assigned to patient MND1 and the other three clusters to the normal, MND, and myopathy groups. Poor performance was also obtained with model 5, where the means of the seven MUAP parameters were used for generating three clusters. Using the same feature set as in model 5 but for $K = 4$, the percentage of correct classifications increased to 83% for the training set and 80% for the evaluation set, shown by model 6. Furthermore, it was decided to exclude patient MND1 from the training set, model 7, and run cluster analysis for $K = 3$. The percentage of correct classifications performance for this model was 86 and 80%, for the training and evaluation sets respectively.

Cluster analysis results for the 14 input models where the mean and standard deviation of the seven MUAP parameters were used are given in Table IV. Diagnostic performance was poor for models 1–3. Comparing models 1 and 2 where the only difference is that in model 2, the number of iterations was increased from 50 to 100, training and evaluation set's performance remained unchanged. In model 3, input data was transformed to its standardized scores; the mean of the feature vector was subtracted from the sample and divided by the feature vector standard deviation. As shown in Table IV, the transformed input data has not helped the K-means algorithm

TABLE IV
K-MEANS CLUSTER ANALYSIS PERFORMANCE WHEN MN AND SD OF THE SEVEN MUAP PARAMETERS WERE USED

					Training	Evaluation						
	No. of inputs	Comments	I*	K	%CCs	%CCs	%FPs	%FNs	SE	SP	RE	PR
1	14		50	3	58	55	17	57	43	83	43	86
2	14		100	3	58	55	17	57	43	83	43	86
3	14	Standardised data	50	3	50	60	14	54	46	86	43	86
4	14	Patient MND1 excluded	50	3	87	85	0	21	79	100	79	100

I* = Number of iterations.

TABLE V
NEURAL NETWORK BACK PROPAGATION EMG MODELS

Model	Architecture	Weights	Gain (η)	Momentum (α)	Epochs	TSS	Training Time* (seconds)		Training	Evaluation						
							One epoch	Total	%CCs	%CCs	%FPs	%FNs	SE	SP	RE	PR
1	14-10-5-3	205	0.01	0.01	17316	0.89	0.124	2147	100	85	0	21	79	100	79	100
2	14-10-5-3	205	0.01	0.1	15745	0.89	0.124	1952	100	85	0	21	79	100	79	100
3	14-10-5-3	205	0.05	0.5	1867	0.89	0.124	231	100	85	0	21	79	100	79	100
4	14-10-5-3	205	0.1	0.5	1333	0.66	0.124	165	100	80	17	21	79	83	79	91
5	14-40-10-3	990	0.01	0.01	3745	0.89	0.529	1981	100	90	0	14	86	100	86	100
6	14-40-10-3	990	0.1	0.1	392	0.86	0.529	207	100	90	0	14	86	100	86	100
7	14-40-10-3	990	0.5	0.5	136	0.89	0.529	72	100	85	0	21	79	100	79	100
8	14-100-10-3	2430	0.01	0.01	2940	0.89	1.3	3822	100	90	0	14	86	100	86	100
9	14-100-10-3	2430	0.1	0.1	279	0.89	1.3	363	100	90	0	14	86	100	86	100
10	14-100-10-3	2430	0.5	0.5	81	0.89	1.3	105	100	90	0	14	86	100	86	100

*Measured on an NCR 3445 PC486 machine running at 33 MHz.

to improve its performance. The performance of model 4 improved when patient MND1 was excluded from the data set and K was set to three. For the 14 input feature vector, the K-means cluster analysis resulted in poorer diagnostic performance for both the training and evaluation sets compared to those of the neural network models, as discussed in the following two sections.

V. NEURAL NETWORK BACK PROPAGATION EMG MODELS

The results of the back propagation neural network models trained with the back propagation learning algorithm are summarized in Table V. The ANN architectures are expressed as strings showing the number of inputs, the number of nodes in the first hidden layer, the second hidden layer, and the output layer, respectively. For all models, the number of inputs is 14 and the number of outputs is three, corresponding to the three groups; NOR, MND, and MYO. Taking into account the problem under consideration, ANN architectures with three layers were used, as these models have been documented as able to draw the boundaries of arbitrarily complex decision regions [17]. The number of weights, the gain or learning rate η, momentum α, and training time are tabulated for each model. During the training phase, an error measure of the closeness of the weights to a solution can be calculated for each pattern (14 input feature vector) that represents a subject in the training set. This measure is used for determining whether a certain subject has been learned by the system, and it is defined by

$$PSS = \sum_{\ell-1}^{M} (y_\ell - d_\ell)^2 \tag{1}$$

where

PSS: Pattern sum of squares.
M: Number of output nodes (three in this case).
y_ℓ: Calculated output.
d_ℓ: Desired output.

The PSS measure is then summed over all patterns to get the total sum of squares or TSS measure

$$\text{TSS} = \sum_{m-1}^{p} \sum_{\ell-1}^{M} (y_{m\ell} - d_{m\ell})^2 \qquad m = 1, \cdots, p \tag{2}$$

where p is the number of training patterns (24 in this case).

The error measure TSS is usually plotted against the number of epochs for showing the learning performance of the model under study. During the learning phase for one epoch, all the 24 patterns were applied at random to the neural net model. Learning was achieved when the value of TSS got very small. For the back propagation models examined, training was stopped when the value of TSS dropped below 0.9. For TSS = 0.9, and number of patterns = 24, PSS = 0.9/24 = 0.0375, on average. For each output node, average error = PSS/3 = 0.0375/3 = 0.0125. The square root of 0.0125

= 0.1118, which gives the average error estimated for each node. The diagnostic performance of the evaluation set was carried out using the classifier performance metrics given in Section II. Percentage of correct classifications, %CC's, for all the models in the training set was 100%.

For the models given in Table V, each parameter of the 14-input feature vector was divided by the mean value of the parameter obtained for the 24 patterns in the training set. Preprocessing of data was carried out on all the patterns of both the training and evaluation sets. A large number of models was investigated for ascertaining how the size of the architecture, the gain η, and momentum α coefficients contribute to the overall performance of a diagnostic model during and after the training phase. At present, no method other than empirical has been proposed for choosing the architecture, η, and α for training feedforward neural networks. Models studied showed that learning of the training set does not necessarily guarantee successful diagnostic behavior on the evaluation set. All the models presented in Table V reached a TSS value below 0.9 and 100% CC's for the training set, with the %CC's for the evaluation set varying between 80 and 90%. The best performance was obtained by those models whose first hidden layer had 40 neurons or more, being the minimum number required for achieving a good diagnostic yield for both the training and evaluation sets. It was not difficult to design a model that learned to identify correctly the 24 patterns of the training set; all the models of Table V could do so. It was not easy, however, to achieve generalization, i.e., the capacity of a neural net to correctly classify unknown cases based on the knowledge that was captured during the training phase.

The set of models 1, 2, 3, and 4 with architecture 14-10-5-3 yielded %CC's between 80 and 85%, as shown in Table V. Comparing models 1 and 2, which were both trained with $\boldsymbol{\eta}$ = 0.01 and $\boldsymbol{\alpha}$ = 0.1 and 0.01, respectively, similar learning and diagnostic performance was obtained. When both the gain $\boldsymbol{\eta}$ and momentum $\boldsymbol{\alpha}$ were increased, as in the case of model 3, faster learning was achieved, with the number of epochs being considerably reduced from 15 745 for model 2 to 1867 for model 3. However, for model 4 where $\boldsymbol{\eta}$ was set even higher (0.1), learning was achieved at a similar number of epochs but with significant oscillatory behavior. In addition, %CC's for the evaluation set dropped to 80%. Models 5, 6, and 7 have the same architecture, 14-40-10-3, but they were trained with different $\boldsymbol{\eta}$ and $\boldsymbol{\alpha}$. It is illustrated again that for higher values of η and α, fewer epochs are required for learning. The learning curves for these models are shown in Fig. 4(a), where the oscillatory behavior of model 7 is clearly shown. Model 7, in addition to the oscillatory behavior, yielded in a poorer %CC's score for the evaluation set. Models 8–10 resulted in %CC's = 90, %FP's = 10, and %FN's = 14. Fig. 4(b) shows the learning behavior and the effect of $\boldsymbol{\eta}$ and $\boldsymbol{\alpha}$ for these models. Evidently, larger architectures can handle high values of η and α without affecting the diagnostic performance of the models, as illustrated by model 10.

Models with small architecture, shown in Table V, required more epochs during training, thus were more demanding in computation time; however, for models with bigger architecture, the number of epochs and training time were reduced. Furthermore, a lower number of epochs and reduced training time were the result of increased values in gain and momentum.

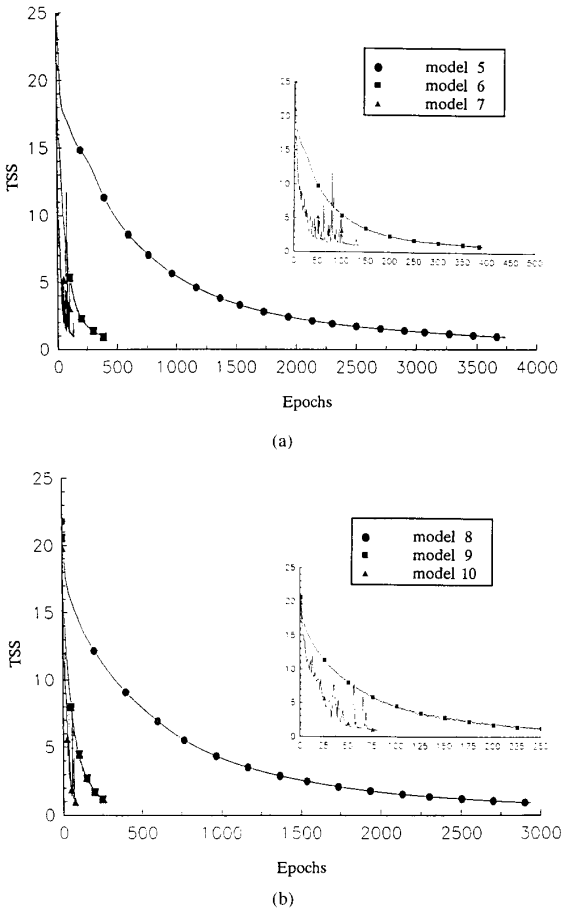

Fig. 4. Learning curves for back propagation EMG models of Table V. (a) Models 5, 6, and 7. (b) Models 8, 9, and 10.

The models shown in Table V were obtained by training the neural network models with preprocessed input data. In general, these models yielded a higher correct classifications score than the back propagation models trained with nonprocessed data [18]. In addition, models of Table V have comparatively lower architectures and required a lower number of epochs for training, thus less computational effort.

An important issue that characterizes the overall performance of the back propagation models presented in Table V regarding subject classification is consistency. Consistency can be addressed in two directions:

1) Of all the models that resulted in the same %CC's, 90% failed to correctly classify the same subjects in all the neural network models. For example, models 5, 6, 8, 9, and 10 of Table V misclassified MND14 as normal and MYO9 as normal. This fact is also revealed by the consistency of the performance metrics.
2) All the models that resulted in 85% CC's incorrectly classified subjects MND14 and MYO9 as normals, as

TABLE VI
SELF-ORGANIZING FEATURE MAP EMG MODELS

Model	No. of Inputs	No. of Classes	Output Grid	Gain factor	Epochs	Training time* (seconds)		Training	Evaluation						
						One epoch	Total	%CCs	%CCs	%FPs	%FNs	SE	SP	RE	PR
1	14	3	6x6	0.09	1550	0.070	108	91	80	17	21	79	83	79	92
2	14	3	6x6	0.5	1550	0.070	108	91	85	0	21	79	100	79	100
3	14	3	6x6	0.9	630	0.070	44	100	85	0	21	79	100	79	100
4	14	3	8x8	0.09	1550	0.112	174	100	80	17	21	79	83	79	92
5	14	3	8x8	0.5	1550	0.112	174	100	85	0	21	79	100	79	100
6	14	3	8x8	0.9	630	0.112	71	100	80	0	28	71	100	71	100
7	14	3	10x10	0.09	1550	0.194	301	100	85	0	21	79	100	79	100
8	14	3	10x10	0.5	1550	0.194	301	100	85	0	21	79	100	79	100
9	14	3	10x10	0.9	630	0.194	122	100	85	0	21	79	100	79	100
10	14	3	12x12	0.09	1550	0.250	387	100	85	0	21	79	100	79	100
11	14	3	12x12	0.5	1550	0.250	387	100	85	0	21	79	100	79	100
12	14	3	12x12	0.9	630	0.250	157	100	85	0	21	79	100	79	100

*Measured on an NCR 3445 PC486 machine running at 33 MHz.

was the case with the above-mentioned models. In addition, they misclassified patient MND10 as being normal.

Subjects MND10 and MND14 both have typical motor neurone disease with bulbar involvement but with less severe involvement of the biceps muscle. Subject MYO9 suffers from polymyositis myopathy. This disease may have foci of inflammation (i.e., areas of muscle distraction) that may not have been picked up in the EMG study.

VI. SELF-ORGANIZING FEATURE MAP EMG MODELS

The neural network models in this system were derived using the Kohonen's self-organizing feature maps algorithm. With this algorithm the training process involves the presentation of pattern vectors from the training set one at a time. A winning neuron (node) is selected in a systematic way after all input vectors are presented. A weight adjustment process takes place by using the neighborhood concept that shrinks over time and a learning coefficient that also decreases with time. After several input vectors are presented, weights will form clusters or vector centers that sample the input space such that the point density function of the vector centers tends to approximate the probability density function of the input vectors [20]. The weights will also be organized such that topologically close output nodes are sensitive to inputs that are physically similar. Thus, the output nodes will be ordered in a natural way.

The results of the self-organizing feature map models that were investigated with no preprocessing of the 14 input feature vector are summarized in Table VI. Models with output grid size: 6 × 6, 8 × 8, 10 × 10, and 12 × 12 were developed. Three different initial gain factors were used with each grid size: 0.09, 0.5, and 0.9. Training for self-organizing feature map EMG models was carried out for 1550 epochs, except for models with gain = 0.9 where the training was stopped at 630 epochs. At each training cycle (epoch), the 24 input patterns were presented at random. It was observed that grid sizes below 6 × 6 were inadequate for producing models with well-separated classes. Models 1 and 2 of Table VI which were trained with gain = 0.09 and 0.5, respectively, could not correctly classify all the cases in the training set, both giving 91% CC's. However, model 3, with a 6 × 6 output grid and gain = 0.9 managed to correctly classify all the subjects in the training set in 630 epochs. Models with output grid size: 8 × 8, 10 × 10, and 12 × 12, could correctly classify all cases in the training set, irrespective of gain factor. Models 4, 5, and 6 were trained with an 8 × 8 output grid and resulted in 80%, 85%, and 80% diagnostic yield, respectively. Models 7–12 resulted in 85% diagnostic yield.

The procedure that was followed for assigning disease classes to the self-organizing feature maps is presented here. For every 14 element feature vector

$$\boldsymbol{x}_n = [\boldsymbol{x}_{1n}\boldsymbol{x}_{2n}\cdots\boldsymbol{x}_{14n}]^T \qquad \boldsymbol{n} = \boldsymbol{1}, \boldsymbol{2}\cdots\boldsymbol{N} \tag{3}$$

where N is the number of patterns in the training set, there is an output node at the grid for which maximum response $\boldsymbol{R}_{\max}$ is caused. This node is assigned the class number of the vector (1 = NOR, 2 = MND, 3 = MYO) and the subject number. Fig. 5(a), which expresses model 3 of Table VI, shows the nodes where maximum response was caused by the subjects in the training set after the completion of the training phase. Nodes with "0 0" values have not been assigned to any class. For this example where the output grid is 6 × 6 (36 output nodes) with a training set of 24 patterns, at least 12 nodes will not be assigned to any pattern. This means that unknown patterns falling on "0 0" nodes will not be diagnosed.

During the next phase, the "0 0" nodes are assigned to one of the classes as follows: the data of each subject in the training set is applied at the input, and the response at a certain "0 0" node is observed

$$\boldsymbol{R}_c = [\boldsymbol{R}_{c1}\boldsymbol{R}_{c2}\cdots\boldsymbol{R}_{cN}]. \tag{4}$$

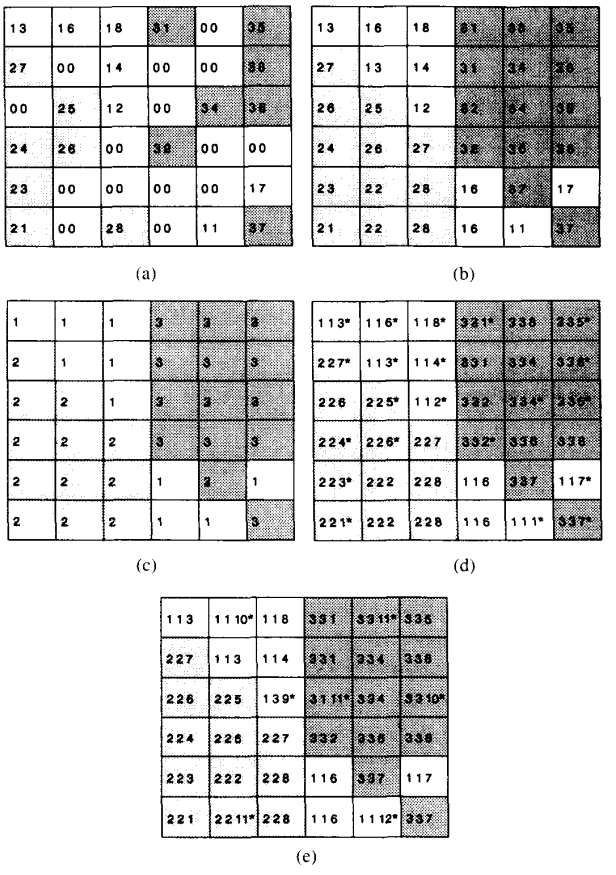

Fig. 5. Self-organizing feature maps of model 3 Table VI. (a) Maximum response map. Legend: 1 3 NOR subject number 3, 0 0 unassigned node. (b) Maximum response map with all nodes assigned. Legend: 2 7 MND subject number 7. (c) Simplified map showing only the classes. Legend: 1 = NOR, 2 = MND, 3 = MYO. (d) Maximum response map for the training set. Legend: 1 1 3* NOR subject number 3 caused maximum response at that node. (e) Maximum response map for the evaluation set. Legend: 1 1 10* NOR subject number 10 is diagnosed correctly, 1 3 9* MYO subject number 9 is diagnosed as NOR.

The class of the subject that causes maximum response $R_{c\max}$ at the node is assigned to the node. This procedure is applied for all the "0 0" nodes until all of them are assigned to a class. Algorithmically, the above procedure can be described as follows:

1) For the "0 0" node c under investigation, compute the response vector R_c;
2) Select the feature vector x_n that gives maximum response $R_{c\max}$; get its class k_m;
3) Assign the class k_m to the node under investigation;
4) Repeat for the next "0 0" node.

The above procedure was applied to the map in Fig. 5(a) of model 3 and the resulting map is shown in Fig. 5(b). A simplified version of the map in Fig. 5(b) is shown in Fig. 5(c) where only the class type is shown. The map in Fig. 5(d) is an integration of the maps in Fig. 5(a) and (b). In this figure, the nodes marked with an "*" are the nodes where the subjects in the training set caused maximum response; for example, node "2 2 4*" means that the node is of class 2, i.e., (MND), and that the 4th MND patient caused maximum response at this node. The diagnosis of the unknown cases in the evaluation set is carried out by applying the 14 element vectors of each subject at the input of a trained neural network model and observing where on the grid the maximum output is caused; the class of the node denotes the diagnostic finding of the system. Correct classification and diagnosis is ascertained when a subject in the evaluation set causes maximum output at a node that belongs to the same class as that of the subject. In Fig. 5(e), the maximum response mapping of the subjects in the evaluation set is shown with an "*." For example, node "1 1 10*" indicates that it belongs to class 1 (NOR) and that subject NOR10 caused maximum response at this node; thus, this subject was correctly diagnosed. However, "1 3 9*" indicates that the node belongs to the normal class and that patient "3 9" (MYO9) was diagnosed as normal, thus incorrectly diagnosed.

Regarding the consistency of the self-organizing feature map models, it was found that all models with 85% diagnostic yield misclassified patients MND10, MND14, and MYO9 as normals, %FP's = 0, and %FN's = 21. All models with 80% diagnostic yield erroneously classified MND10, MND14, and MYO9 as normals and, in addition, they misclassified NOR11 as myopathic with %FP's = 17, and %FN's = 21.

The self-organizing feature maps system compared to the back propagation neural network system has the advantage of the results being presented pictorially. For example, in Fig. 5(e), row 6, column 2, "2 2 11*," indicates that patient MND11 was correctly diagnosed. With this system one can easily relate a certain patient with another patient, find boundary cases, and observe the mapping of a patient over serial examinations. Training effort for the self-organizing feature map models was significantly reduced as compared to the momentum back propagation models, see Tables V and VI.

VII. Conclusions

Neural network EMG diagnostic models in conjunction with quantitative analysis provide an integrated solution to the problem of automated EMG evaluation. This approach is very desirable because it minimizes observer bias, facilitates comparison of results across individuals and different methodologies, and more importantly, provides useful information for helping the physician in reaching a more accurate diagnosis. It should be emphasized that if the disease process is advanced and the electrophysiological abnormalities are many and obvious, although automated EMG analysis might be of less importance diagnostically, it may be useful for detecting and characterizing changes on a series of examinations [26]. On the other hand, the application of computer-aided EMG analysis is very important in detecting pathology in those early or mild cases of a disease where the electrophysiological abnormalities are relatively slight and may escape accurate diagnosis. In this paper, we have presented how artificial neural network models can be applied in the assessment of patients suffering with neuromuscular disorders based on EMG. The diagnostic performance of neural network models

investigated is on the order of 80–90% for models trained with the back propagation algorithm and 80% for models trained with the Kohonen's self-organizing feature maps algorithm. The K-means cluster analysis algorithm gave poorer performance.

Neural network EMG models trained with the individual parameters for each MUAP set forming a 140 input feature vector (20 MUAP sets $\times$ seven parameters) were also studied [27] for the same group of patients. Comparing 14 input and 140 input ANN models, it can be concluded that although both sets of models achieved a similar diagnostic performance, the 14 input models require a considerably higher number of epochs to achieve learning. Recently, Genetics Based Machine Learning (GBML) models have been developed to classify normal, MND, and myopathy subjects based on EMG data [28]. Diagnostic performance of GBML and neural network back propagation and self-organized feature map models was found to be similar. However, training effort for GBML models was reduced as compared to both the back propagation and the self-organized feature maps ANN models.

Future work should take into account the severity of the disease (mild, moderate, severe, and chronic states), another aspect of EMG diagnosis that needs to be investigated. Furthermore, data from more patients, more muscles, and more neuromuscular diseases have to be included in the system. However, diagnosis of neuromuscular diseases, in addition to neurophysiological findings, is based on patient's clinical assessment, muscle biopsy, biochemical findings, and genetic and molecular genetic findings. Presently, no expert system or any other intelligent system exists for the diagnosis of neuromuscular disorders taking into account all of the above disciplines. It is suggested that the ultimate goal would be to develop a multidiscipline computer-aided system for medical diagnosis of these disorders. The system should be able to process data in the form of images, signals, measurements, signs, and symptoms. Such a system could be developed based on procedures applied in the early and accurate diagnosis of the clinical types and stages of neuromuscular disorders, their clinical subtypes, and variants.

ACKNOWLEDGMENT

This work was carried out on an NCR 3445 computer system donated to CING through NCR Cyprus. Furthermore, the authors would like to express sincere thanks to E. Polycarpou, technical assistant.

REFERENCES

[1] C. K. Jablecki, C. F. Bolton, W. G. Bradley, W. F. Brown, F. Buchthal, R. Q. Cracco, E. W. Johnson, G. H. Kraft, E. H. Lamberg, H. O. Lueders, D. M. Ma, J. A. Simpson, and E. V. Stalberg, *A Glossary of Terms Used in Clinical Electromyography*, 2nd ed. Nomenclature Committee of the American Association of Electromyography and Electrodiagnosis, 1987.

[2] F. Buchthal, P. Pinelli, and P. Rosenfalck, "Action potential parameters in normal human muscle and their physiological determinations," *Acta. Physiol. Scand.*, vol. 32, pp. 219–229, 1954.

[3] F. Buchthal, C. Guld, and P. Rosenfalck, "Action potential parameters in normal human muscle and their dependence on physical variables," *Acta Physiol. Scand.*, vol. 32, pp. 200–215, 1954.

[4] F. Buchthal, *An Introduction to Electromyography*. Copenhagen: Gyldendal, 1957.

[5] E. Stalberg, S. Andreassen, B. Falck, H. Lang, A. Rosenfalck, and W. Trojaborg, "Quantitative analysis of individual motor unit potentials: A proposition for standardized terminology and criteria for measurement," *J. Clin. Neurophysiol.*, vol. 3, no. 4, pp. 313–348, 1986.

[6] K. J. Blinowska, I. Hausmanowa-Petrusewicz, A. Miller-Larsson, and J. Zachara, "The analysis of single EMG potentials by means of multivariate methods," *Electromyogr. Clin. Neurophysiol.*, vol. 20, pp. 105–123, 1980.

[7] J. L. Coatrieux, P. Toulouse, B. Rouvrais, and R. Le Bars, "Automatic classification of electromyographic signals," *EEG Clin. Neurophysiol.*, vol. 55, pp. 333–341, 1983.

[8] B. Rouvrais, P. Toulouse, J. L. Coatrieux, and R. Le Bars, "A possible method of automatic electromyographic analysis and diagnosis on line," *Electromyogr. Clin. Neurophysiol.*, vol. 23, pp. 457–470, 1983.

[9] P. Toulouse, J. L. Coatrieux, and B. Le Marec, "An attempt to differentiate female relatives of Duchenne type dystrophy from healthy subjects using an automatic EMG analysis," *J. Neurolog. Sci.*, vol. 67, pp. 45–55, 1985.

[10] S. K. Andersen, S. Andreassen, and M. Woldbye, "Knowledge representation for diagnosis and test planning in the domain of EMG," in *Proc. 7th Eur. Conf. Artificial Intell.*, Brighton, U.K., pp. 357–368, 1986.

[11] S. Andreassen, S. K. Andersen, F. V. Jensen, M. Woldbye, A. Rosenfalck, B. Falck, U. Kjaerluff, and A. R. Sorensen, "MUNIN—An expert system for EMG," *Electroenceph. Clin. Neurophysiol.*, vol. 66, no. S4, 1987.

[12] S. Andreassen, F. Jensen, S. K. Andersen, B. Falck, U. Kjaerulff, M. Woldbye, A. R. Sorensen, A. Rosenfalck, and J. Frank, "MUNIN—An expert EMG assistant," in *Computer Aided Electromyography and Expert Systems*, J. E. Desmedt, Ed. New York: Elsevier Science Publishers B.V., 1989, pp. 255–277.

[13] A. Fuglsang-Frederiksen and S. M. Jeppesen, "A rule-based EMG expert system for diagnosing neuromuscular disorders," in *Computer Aided Electromyography and Expert Systems*, J. E. Desmedt, Ed. New York: Elsevier Science Publishers B.V., 1989, pp. 289–296.

[14] A. Fuglsang-Frederiksen, J. Ronager, and S. Vingtoft, "A plan-test-diagnose expert system for EMG: KANDID," *J. Neurolog. Sci.*, vol. 98 (suppl.), p. 150, 1990.

[15] P. W. Jamieson, "Computerized interpretation of electromyographic data," *Electroencephalogr. Clin. Neurophysiol.*, vol. 75, p. 392, 1990.

[16] ——, "A model for diagnosing and explaining multiple disorders," *Comput. Biomed. Res.*, vol. 24, pp. 307–320, 1991.

[17] R. P. Lippmann, "An introduction to computing with neural nets," *IEEE ASSP Mag.*, Apr. 4–22, 1987.

[18] C. S. Pattichis, "Artificial neural networks in clinical electromyography," Ph.D. dissertation, Dep. Elec. Eng., Queen Mary and Westfield College, University of London, U.K., Mar. 1992.

[19] D. Rumelhart, G. Hinton, and G. Williams, "Learning internal representations by error propagation," in *Parallel Distributed Processing: Explorations in the Microstructures of Cognition*, vol. 1, D. Rumelhart and J. McCleland, Eds. Cambridge, MA: MIT Press, 1986, pp. 318–362.

[20] T. Kohonen, *Self-Organization and Associative Memory*. Berlin: Springer-Verlag, 1984.

[21] J. T. Tou and R. C. Gonzalez, *Pattern Recognition Principles*. New York: Addison-Wesley, 1974.

[22] R. C. Eberchart and R. W. Dobbins, *Neural Network PC Tools, A Practical Guide*. New York: Academic, 1990.

[23] J. Walton, "A simple classification of neuromuscular diseases," *Neuro-Muscular Diseases News Bullet.*, Mar. 1992.

[24] W. Trojaborg, "Motor unit disorders and myopathies," in *A Textbook of Clinical Neurophysiology*, M. A. Halliday, R. S. Butler, and R. Paul, Eds. New York: Wiley, 1987, pp. 417–438.

[25] C. N. Schizas, C. S. Pattichis, R. R. Livesay, I. S. Schofield, K. X. Lazarou, and L. T. Middleton, "Unsupervised learning in computer aided macro electromyography," in *Computer-Based Medical Systems, Proc. 4th Annu. IEEE Sympos.*, I. N. Bankman and J. E. Tsitlik, Eds., pp. 305–312, 1991.

[26] L. J. Dorfman and K. C. McGill, "AAEE minimonograph #29: Automatic quantitative electromyography," *Muscle and Nerve*, vol. 11, pp. 804–818, 1988.

[27] C. S. Pattichis, C. N. Schizas, L. T. Middleton, and W. F. Fincham, "Computer aided clinical electromyography," in *Proc. 12th Annu. Int. Conf. IEEE EMBS*, P. C. Pedersen and B. Onaral, Eds., pp. 2229–2231, 1990.

[28] C. N. Schizas, C. S. Pattichis, and L. T. Middleton, "Neural networks, genetic algorithms, and K-means algorithm: In search of data classification," in *Combination of Genetic Algorithms and Neural Networks*, D. Whitley and D. Schaffer, Eds. Piscataway, NJ: IEEE Computer Society Press, 1992, pp. 201–222.

Constantinos S. Pattichis (S'83–M'88) was born in Nicosia, Cyprus in 1959. He received the B.Sc. degree in electrical engineering from the University of New Brunswick, Canada in 1983, the M.Sc. degree in biomedical engineering from the University of Texas at Austin in 1984, the M.Sc. degree in neurophysiology from the University of Newcastle upon Tyne, U.K. in 1988, and the Ph.D. in electronic engineering from the University of London, U.K. in 1992.

From 1985–1992, he was working with the Cyprus Institute of Neurology and Genetics as a Research Scientist and later on as Senior Scientist in the area of neurophysiology and computer research systems. He is currently a Lecturer in the Department of Computer Science at the University of Cyprus.

Dr. Pattichis is the recipient of the 1994 European Community "Marie-Curie" fellowship. His research interests include biosignal analysis, medical imaging, artificial neural networks, and genetic algorithms.

Christos N. Schizas (M'78–SM'91) was born in Cyprus in 1952. He received the B.Sc. in electronics and the Ph.D. in systems theory from Queen Mary College, University of London, in 1978 and 1981, respectively, and the M.B.A. from the University of Indianapolis in 1988.

After completing research studies, he worked for three years as a postdoctoral fellow of computer information systems at the University of London. In 1985, he joined the Higher Technical Institute in Cyprus as a Lecturer in Computer Science. In 1987, he formed a research team for studying artificial neural networks and their applications in medicine. In 1988, he became the Director of Computer Systems and Artificial Intelligence Research at the Cyprus Institute of Neurology and Genetics. In 1989, he joined the University of Indianapolis as a Visiting Professor and later on as a Professor of Computer Information Systems. In 1991, he joined the Department of Computer Science of the newly established University of Cyprus, where he currently serves as Interim Chair of the Department. His research interests are artificial neural networks, genetic algorithms, computer applications in medicine, and diagnostic systems.

Dr. Schizas received the William Lincoln Shelley Award of the University of London for his research work. He is on the International Scientific Committee of the IEEE-EMBS, a founding member of the IEEE Cyprus Section, and a Fellow of IEE and BCS.

Lefkos T. Middleton received the medical doctorate degree in 1976 from the University of Strassbourg, France, and completed a specialization in neurology and neurophysiology in France, with a year at Guy's Hospital, London.

He was a Visiting Professor at Columbia University and a Fellow at the Neurological Institute of New York in 1980–1981. He is currently a Consultant Neurologist and the Chairman of the Cyprus Institute of Neurology and Genetics in Nicosia, Cyprus. He directs research in the field of neuromuscular diseases with emphasis in quantitative electromyography.